Check for updates

Green synthesis of silver nanoplates using the special category of plant leaves showing the lotus effect†

Sangeeta Agarwal, [ID][a] Manisha Gogoi,[a] Smritirekha Talukdar,[a] Pinky Bora,[b] Tarun Kumar Basumatary[b] and N. Nirjanta Devi[b]

This paper reports the first ever green synthesis of silver nanoplates using plant leaves having the special feature of showing the lotus effect. *Eichhornia crassipes* and *Colocasia esculenta* plant leaves were chosen for the purpose. The aqueous leaf extract of these plants was used as a reducing as well as stabilizing agent in the hydrothermal synthesis of silver nanoplates using silver nitrate as the precursor. Well dispersed silver nanoplates were formed. The appearance of two SPR (Surface Plasmon Resonance) bands corresponding to in-plane and out of plane vibration confirmed the formation of anisotropic nanostructures. The blue shift in peaks of the nanostructures in UV-visible spectra gave information about the stability of the nanoplates with time. Dynamic Light Scattering (DLS) and powder XRD were used to evaluate the ultimate average diameter and crystal structure of these nanostructures respectively. FESEM/EDX and HRTEM/SAED images also confirmed the formation of silver nanoplates. The FT-IR spectra helped to identify the reducing and stabilizing component of plant leaves extract in the formation of 2-D nanostructures. Preliminary antibacterial activity was examined using these nanoplates. A significant zone of inhibition was observed for *S. aureus*, a Gram positive bacterium.

Introduction

Nanoplates are Surface Plasmon Resonant (SPR) platelet-shaped nanoparticles. Precise control of the plate diameter and thickness can help in tuning a nanoplate's optical resonance at specific wavelengths (450–1000 nm). Ag nanoplates were first synthesized by Mirkin and co-workers by photo-induced chemical reaction.[1] Since then many other methods like chemical reduction, sonochemical route, bacterial synthesis *etc.* have been proposed for the synthesis of silver nanoplates. Isabel Pastoriza-Santos and Luis M. Liz-Marzan published an overview on research on the synthesis, properties and applications of silver nanoplates in 2008. Till then only wet chemical and nanosphere lithography methods were in use for the synthesis of silver nanoplates.[2] Zao *et al.* synthesized silver nanoplates in 2011, with average thickness about 5 nm and average tuneable size from 40 to 500 nm, *via* a simple room-temperature solution-phase chemical reduction method in the

presence of appropriate concentration of trisodium citrate and silver seeds.[3] In 2011, Zhang *et al.* identified the critical role of hydrogen peroxide in the chemical reduction method of synthesizing triangular nanoplates.[4] Shahzad *et al.* put forward a simple, fast and room temperature aqueous-phase chemical route in 2018 to synthesize silver nanoplates with controllable sizes from 1–17 μm.[5] Dang *et al.* tried to synthesize silver nanoparticles and nanoplates from silver nitrate by using PVP (poly vinyl pyrrolidone) as both size controller and capping agent with H_2O_2 and trisodium citrate to control synthesis of nanoplates.[6] Green synthesis of metal nanoparticles is always favoured over the chemical synthesis.[7] Ramanathan *et al.* in 2010 reported the first ever biological synthesis of thin silver nanoplates from a silver resistant bacterium, *Morganella psychrotolerans* by controlling the growth kinetics of the bacteria and reaction parameters.[8] A large number of papers report the synthesis of spherical silver nanoparticles using different plant extracts. But, there is no literature report on the synthesis of silver nanoplates using any plant extract. Since nanoplates have excellent optical properties, these 2-D structures find applications in surface-enhanced Raman scattering (SERS), photovoltaics, molecular detection, photo thermal cancer therapies and in catalysis.[5] Silver nanoplates have been reported to possess improved antimicrobial property compared to the spherical and rod shaped silver nanoparticles. It has been proposed that nanoscale size and the presence of {111} basal plane improves the antimicrobial property in nanoplates.[9] A coating and

[a]Department of Chemistry, Cotton University, Pan Bazar, Guwahati-781001, Assam, India. E-mail: agarwalsangee@gmail.com

[b]Department of Molecular Biology and Biotechnology (MBBT), Cotton University, Pan Bazar, Guwahati-781001, Assam, India

Fig. 1 Lotus effect with epicuticular wax covered surface nano-structures responsible for super hydrophobicity of leaf surface.[12]

Fig. 2 Leaves of (a) *Eichhornia crassipes* (b) *Colocasia esculenta* and (c) *Nelumbo nucifera*.

functionalization of coatings may further enhance the antimicrobial property of the silver nanoplates. Ichimaru *et al.* have reported the improved antimicrobial property of gold coated triangular silver nanoplates.[10] Djafari *et al.* have recently reported the synthesis and characterization of triangular nanoplates. They have used functionalized silica coating on silver nanoplates in order to improve the antibacterial activity of silver nanoplates.[11]

Lotus leaves, an aquatic plant of Asian origin, do not get wet and form spherical drops when they come into contact with water on their surface. This allows the water droplets to slide freely taking all dirt with it and keeping the leaf clean and dry. This "self-cleaning" effect is called the Lotus effect and is found in many other plant species (Fig. 1). The reason of super hydrophobic surface is the nano scale surface layer structures and epicuticular wax crystals covered over the surface that repel water droplets.[12,13]

We report here the first ever green synthesis of silver nanoplates using plant leaf extract of *Eichhornia crassipes* and *Colocasia esculenta*. Water hyacinth (*Eichhornia crassipes*) is considered as the notorious aquatic weed present all over the world. The leaves of the plant contain potassium, calcium and silicon as well as numerous secondary metabolic and phytochemicals like phenalenone compounds, alkaloids, flavonoids, phenols, sterols, terpenoids and anthoquinones.[14,15] The leaves of *Eichhornia crassipes* plant also show lotus effect. *Colocasia esculenta* is a traditionally used tropical plant most commonly known as taro. A recent study has revealed honeycomb-like microstructures on the taro leaf, which makes the leaf super hydrophobic.[16] A wide range of chemical compounds including flavonoids, steroids, calcium oxalate are reported to be present in taro leaves.[17]

The leaves extract of these two plants have been used for the synthesis and stabilization of silver nanoplates. The stability of these nanoplates with time and preliminary antimicrobial activity of these nanoplates have also been assessed.

Material and methods

The materials used in this work were fresh water hyacinth (*Eichhornia crassipes*) leaves which were collected from local water bodies of Sibsagar, Assam (India) and fresh leaves of taro (*Colocasia esculenta*) collected from Ganesh nagar, Guwahati, Assam. Lotus leaves (*Nelumbo nucifera*) were also collected from the local market of Panbazar, Guwahati. Silver nitrate was purchased from Merck Life Science Pvt. Ltd., Mumbai, India.
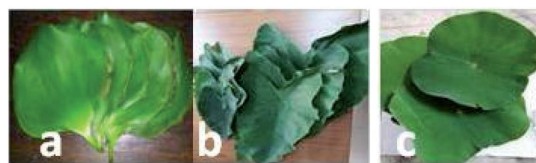
Gallic acid and quercetin were purchased from Alfa Aesar. The chemicals required for antibacterial activity *i.e.* Mueller-Hinton agar, DMSO (dimethyl sulphoxide), tetracycline *etc.* were purchased from Himedia Pvt. Ltd. (Mumbai, India).

A simple hydrothermal process was used to synthesize silver nanoplates. Stirring of the reacting solution was done on a magnetic stirrer equipped with hot plate. The resulting solution was centrifuged using REMI centrifuge machine. UV-visible spectra were recorded on Shimadzu UV-2600 spectrophotometer in the wavelength range of 200–1100 nm. The FT-IR (Fourier Transform Infra Red) spectra were recorded using ALPHA Bruker FT-IR spectrophotometer in the wave number range 4000 cm^{-1} to 500 cm^{-1} using KBr pellet method. The Powder X-ray diffraction patterns of the silver nanoparticles synthesized using *Eichhornia crassipes* were recorded in 2θ range 5°–90° on a D8-ADVANCE Bruker Discover powder diffraction instrument using Cu-Kα radiation. The powder X-ray diffraction patterns of the synthesized silver nanoparticles using *Colocasia esculenta* were recorded in a Philips X'Pert Pro powder X-ray diffractometer. DLS (Dynamic Light Scattering) analysis was performed in a Malvern Zetasizer Nano series compact scattering spectrometer. FESEM (Field Emission Scanning Electron Microscope) images were recorded in a ZEISS SIGMA VP field emission scanning electron microscope and ZEISS SIGMA 300 FESEM instrument. HRTEM/SAED (High Resolution Transmission Electron Microscope/Selected Area Electron Diffraction) analysis was performed using a suspension of silver nanoplates in propan-2-ol dried on a carbon coated Cu grid and images were recorded on a JEOL JEM-2100 electron microscope operating at an accelerating voltage of 200 kV. The particle size of nanoplates was calculated with the help of Image-J software. The SAED pattern was indexed by standard method. Antibacterial activities of the synthesized silver nanoplates against *Escherichia coli*, *B. subtilis* and *Staphylococcus aureus* were investigated at different concentrations of silver nanoplate's solution using well diffusion method with minor modifications.[9]
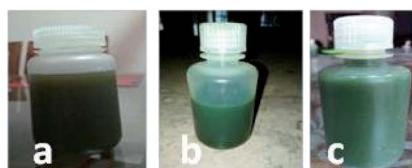

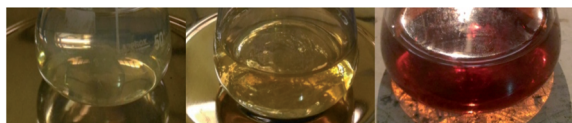Fig. 3 Extract of leaves of (a) *Eichhornia crassipes* (b) *Colocasia esculenta* and (c) *Nelumbo nucifera*.

Fig. 4 Successive colour changes with time during the synthesis of silver nanoplates using leaves extract of *Eichhornia crassipes*.

Synthesis of silver nanoplates

25 g of fresh plant leaves of *Eichhornia crassipes* (Fig. 2a) were crushed and boiled in 200 mL of distilled water at 80 °C for one hour. The extract was then cooled and filtered using Whatman filter paper No. 1. The filtrate was poured in containers and stored in refrigerator (Fig. 3a). 50 mL of 1 mM solution of AgNO$_3$ in distilled water was stirred and heated up to 60 °C on a hot plate of magnetic stirrer. 25 mL of *Eichhornia crassipes* leaf extract was added and stirring was continued for another 1 hour at 60 °C. The reaction mixture was then cooled centrifuged and the UV-visible spectra were recorded immediately after reaction as well as after certain hours and days intervals.

The colour of the reaction mixture changes from yellow to reddish orange with time (Fig. 4). The solution was allowed to stand and the UV-visible spectra were recorded regularly for 35 days in order to observe the stability of nanoplates. The synthesis process was repeated varying the temperature and concentration of *Eichhornia crassipes* leaves extract and aqueous solution of AgNO$_3$. At temperature lower than 60 °C, the intensity of the UV-Vis peaks were comparatively low. The experiment was also carried out taking 1 : 1 ratio of AgNO$_3$ solution and the leaf extract. Though silver nanoplates were formed in this case also, there was poor intensity of the UV-Vis peaks (Fig. S1†) and the colour of final solution was also darkest brown with some turbidity showing agglomeration (Fig. S2†). The best results were obtained at 1 : 2 ratio of leaves extract of the above mentioned concentrations and AgNO$_3$.

Similar experiments were carried out to synthesize silver nanoplates using aqueous leaves extract of *Colocasia esculenta* and *Nelumbo nucifera* separately. The temperature and concentrations were varied in series of experiments. Interestingly, the best results were obtained with 1 : 2 ratio of aqueous extract of leaves and AgNO$_3$ solution. The patterns of colour changes in each of these two cases are shown in Fig. S3 and S4.† The same optimal conditions of temperature and concentration in experiments using each of the three types of the leaves may be due to super hydrophobic surfaces of the leaves having very near values of the contact angles (162° for *Nelumbo nucifera*, 164° for *Colocasia esculenta* and 154° for *Eichhornia crassipes*) and involvement of similar chemicals in the reduction and stabilization of silver nanoplates during the synthesis.

Results and discussion

The UV-visible spectra of the reaction mixture as a function of time were recorded in order to follow the stability and formation of silver nanoplates.
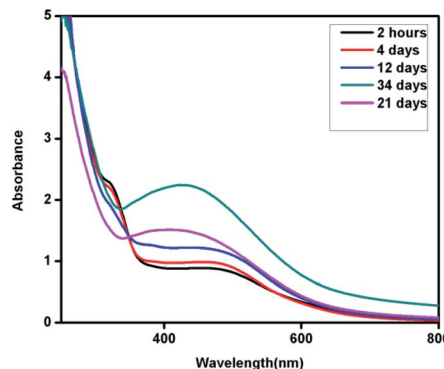

Fig. 5 UV-Vis spectra of silver nanoplates synthesized using *Eichhornia crassipes* leaf extract as a function of time.

According to Mie's theory, only a single Surface Plasmon Resonance (SPR) band at about 400 nm is observed in the absorption spectra of spherical silver nanoparticles. The anisotropic structures may give rise to two or more surface plasmon resonance bands depending on the shape of the particles.[11]

Interestingly, in the absorption spectra of the synthesized nano structures using *Eichhornia crassipes* leaf extract, two SPR bands were observed instead of one (Fig. 5). This shows the anisotropic behaviour of the synthesized nanostructures. One of the SPR band was found to be centred at 526 nm expanded broadly in between 400–600 nm range, while other broad peak around 320 nm. The SPR band at 526 nm which may be due to out of plane oscillation, shifts towards shorter wavelength with increase in intensity while the band at 320 nm, attributed to in-plane oscillation becomes less intense with time. The appearance of two SPR bands indicates the formation of silver nanoplates. Chen and Carroll have discussed different aspects of formation of silver nanoplates and have shown that the number of UV-Vis peaks may be two or more depending upon the shape of the nanoplates.[18] Pastoriza-Santos and Liz-Marzán have also supported the presence of two or more UV-Vis peaks for silver nanoplates with a comparative theoretical study and experimental results.[19]

The blue shift in the higher wavelength SPR band from λ_{max} 526 nm to 407 nm with time indicates that the nanoplates are
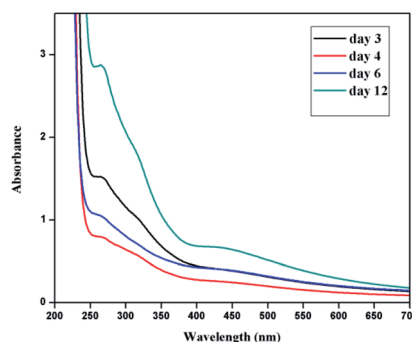

Fig. 6 UV-Vis spectra of silver nanoplates synthesized using *Colocasia esculenta* leaf extract as a function of time.

sensitive to environment and become smaller with time. This may be due to dissolution of edges and reduction in the size of the synthesized silver nanoplates with time. The hypsochromic shift in the UV-Vis spectra can be followed from Fig. 5.

Similarly silver nanoplates synthesized using *Colocasia esculenta* leaf extract shows two peaks, one centred in the wavelength range 400–600 nm (attributed to out of plane oscillation) and other centred at 312 nm (attributed to in plane oscillation) as shown in Fig. 6.

The use of *Nelumbo nucifera* leaves extract in the synthesis of silver nanoplates followed the same results as revealed by UV Vis spectra (Fig. S5†). Abou Talib and Hui-Fen-Wu have reported the use of *Nelumbo nucifera* leaf extract in the synthesis of silver nanoparticles. The pattern of UV Vis spectra reported by them is in consistent with the results that we have got in our work. They have reported UV Vis spectra drawn starting from wavelength 350 nm. The surface plasmon band at around 320 nm due to in-plane oscillation must have cut off in their spectra as the nanostructures they had synthesized were actually nanoplates. This is in consistent with our observation that nanoplates and not spherical nanoparticles are formed when we use super hydrophobic leaves *i.e.* the plant leaves which show lotus effect.[20] Supraja *et al.* have also claimed to synthesize silver nanoparticles using the extract of lotus leaves, but the UV Vis spectrum in their paper also reveals the formation of nanoplates.[21]

FT-IR Spectra were recorded both for dried powder of *Eichhornia crassipes* leaves and silver nanoplates synthesized using the leaves extract (Fig. 7a). The purpose was to detect major phytochemicals responsible for the reduction of the metal and stabilization during the synthesis of silver nanoplates. A strong and broad band between 3800 to 2500 cm^{-1} has been assigned to –OH stretching vibration and a shoulder at 1710 cm^{-1} due to aromatic –CO stretching vibration indicating the presence of
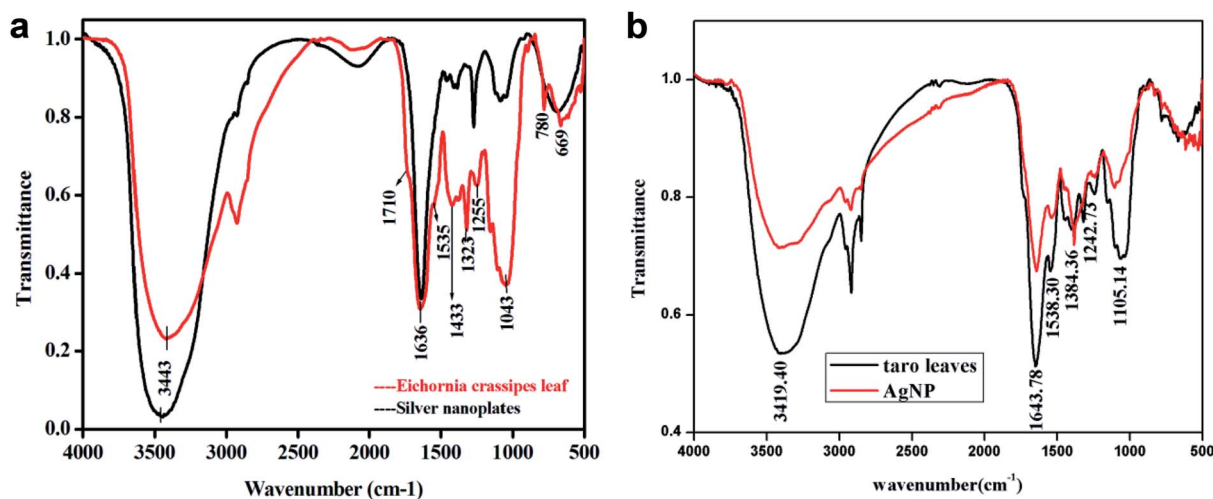

Fig. 7 (a) FT–IR spectra of the *Eichhornia crassipes* leaf extract and the silver nanoplates synthesized using it. (b) FT–IR spectra of the *Colocasia esculenta* leaf extract and the silver nanoplates synthesized using it.
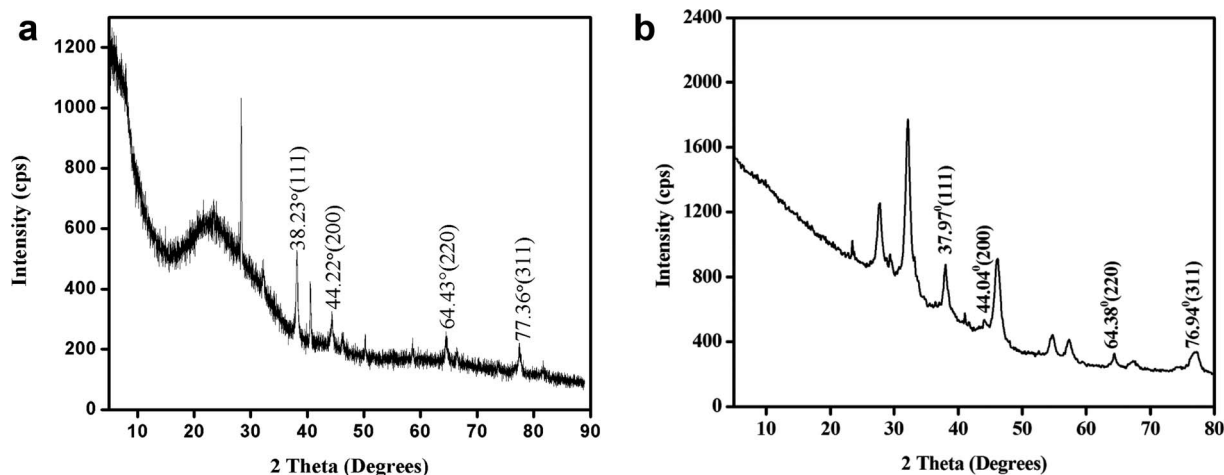

Fig. 8 (a) Powder XRD of silver nanoplates synthesized using *Eichhornia crassipes* leaf extract. (b) Powder XRD of silver nanoplates synthesized using *Colocasia esculenta* leaf extract.

aromatic carboxylic acid group in gallic acid.[22] The band at 2934 cm^{-1} has been assigned to C–H stretching vibration and shoulder at 1730 cm^{-1} due to ketonic–CO group. The band at 1643 cm^{-1} is due to quercetin,[23] a flavanoid present in the leaf extract of W. H. plant (*Eichhornia crassipes*) and no change in its intensity shows that this compound may be responsible for the stabilization of nanoplates. The band at 1636 cm^{-1} is due to aromatic C=C stretching vibration which may also cover –CO stretch due to presence of amide group. The bands at 1616 cm^{-1} (as shoulder), 1535 cm^{-1} and 1433 cm^{-1} are assigned to stretching vibrations due to C–C bonds in aromatic ring. Other peaks in 1250 to 500 cm^{-1} range are due to C–H bending in aromatic ring, =C–H and =CH$_2$ out of plane bending, –OH bending, C–H deformation *etc.* which have significantly reduced in intensity after the formation of silver nanoplates. The band at 1255 cm^{-1} has been assigned to secondary alcohol C–O stretching vibration for nonacosan-10-ol with –OH stretching covered in the broad band centred at 3443 cm^{-1}. The –OH stretch for nonacosanediols which nearly fall in 3600 cm^{-1}, has also been covered by the broad band extending from 3800 to 2500 cm^{-1}.

Similar results were observed for taro (*Colocasia esculenta*) leaves as given in Fig. 7b. FT-IR of both plant leaves show the presence of nonacosanediols and nonacosan-10-ol which are the constituents of the wax covering the surface nanostructures of the leaves.[24]

The powder XRD pattern in Fig. 8a and b shows the peaks at 2θ values 38.23°, 44.22°, 64.43°, 77.36° corresponding to the lattice plane (111), (200), (220) and (311) assigned to face centred cubic structure of silver nanoplates (JCPDS file number 87-717). Similarly powder XRD pattern in Fig. 8b also corresponds to the same structure of silver nanoplates. Extra peaks observed in the XRD pattern are due to some crystalline organic phases (like nonacosanediols and nonacosan-10-ol) present in the leaves of both types of plants.[13,25]

The average crystallite size of the silver nanoplates was estimated using Debye–Scherrer equation:

$$D = \frac{K\lambda}{\beta \cos\theta}$$

where D is the crystallite size, K is a constant having value 0.9, λ is the wavelength of the X-rays used having the value 1.54 A°. By determining β, the FWHM (fixed width at half maximum) value of the most intense (111) Bragg's reflection, the estimated average size of the nanoplates was 22.41 nm which were synthesized using *Eichhornia crassipes* plant leaves extract and
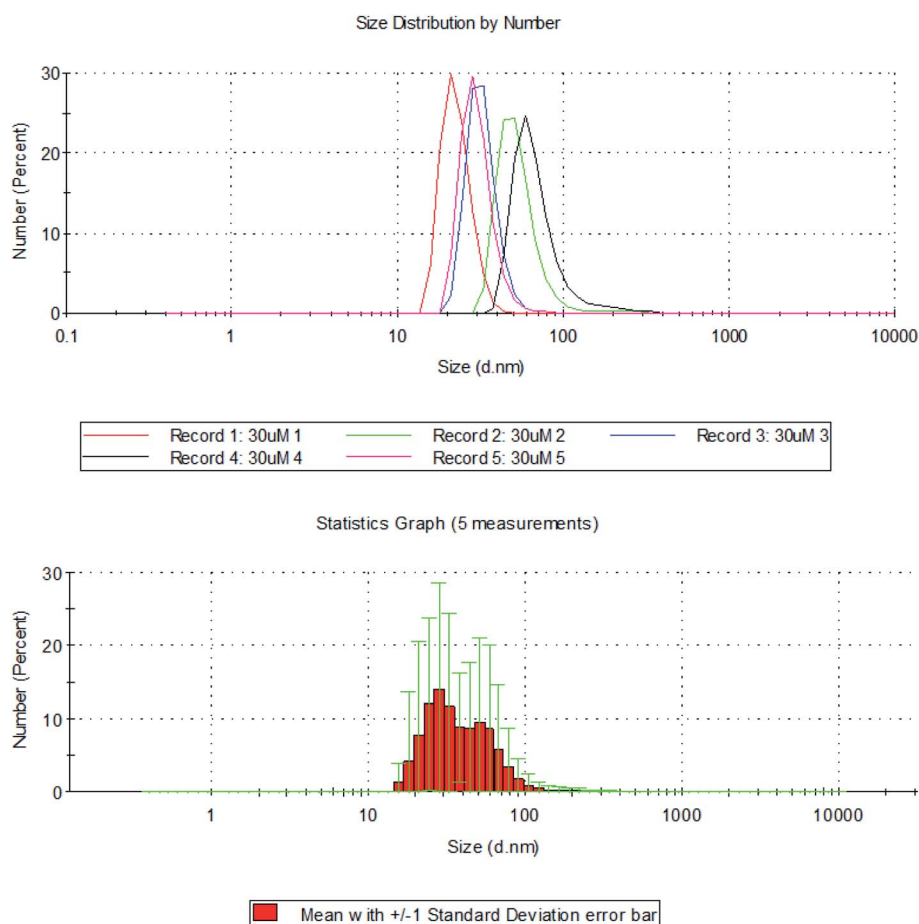

Fig. 9 Hydrodynamic diameter of silver nanoplates measured using DLS with standard deviation graph for size distribution of silver nanoplates using DLS.

11.34 nm for the nanoplates synthesized using *Colocasia esculenta* leaves extract.

The hydrodynamic diameter of silver nanoplates was determined using DLS (Dynamic Light Scattering). The size distribution of silver nanoplates ranges from 10–150 nm. It was observed that maximum percentage (99.8%) of the particles were of size 22.6 (*d.* nm). About 0.2% of the silver nanoplates were of size 91.97 (*d.* nm). The *Z*-average value of the silver nanoplates synthesized from *Eichhornia crassipes* is 135.6 (*d.* nm).

Sizes and shapes of metal nanoparticles are influenced by a number of factors including pH, precursor concentration, reductant concentration, time of incubation, temperature as well as method of preparation. The size distribution image of the synthesized silver nanoplates and the standard deviation graph are shown in Fig. 9. The DLS report regarding the particle size is in consistent with the average size of particles obtained from Debye Scherrer equation.

FESEM images and EDS (Energy Dispersive X-ray Spectrum) data of the freshly prepared samples (Fig. 10) clearly shows the formation of well dispersed hexagon shaped silver nanoplates (size < 200 nm) stabilized by coating of Si. The EDX report shows the presence of Ag and Si. Silicon is reported to be present as one of the constituent chemical in the *Eichhornia crassipes* leaves extract by Lara Serrano *et al.*[14] The formation of nanoplates is also in consistent with UV-Vis spectra analysis. The FESEM images were recorded within two days of the synthesis to confirm that initially larger hexagonal silver nanoplates were formed. The synthesized nanoplates are sensitive to the surrounding environment resulting in dissolution of the edges and the ultimate size of the nanoplates remains approx. 22.6 nm. This is the reason why the powder XRD and DLS report which were recorded quite after some days from the synthesis of the nanoplates are revealing the ultimate size (22.6 nm) of the nanoplates and not the initial size (approx. 150 nm) of the nanoplates. The blue shift in UV-Vis spectra also confirms the reduction in the size of nanoplates with time.
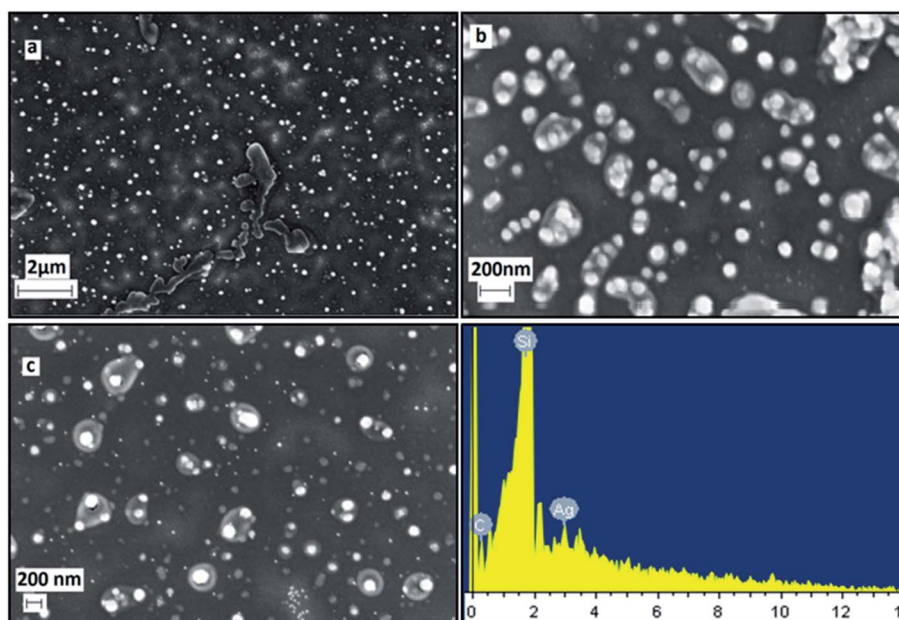

Fig. 10 FESEM/EDX images of freshly synthesized silver nanoplates using *Eichhornia crassipes* leaf extract at different scales (a, b, c).
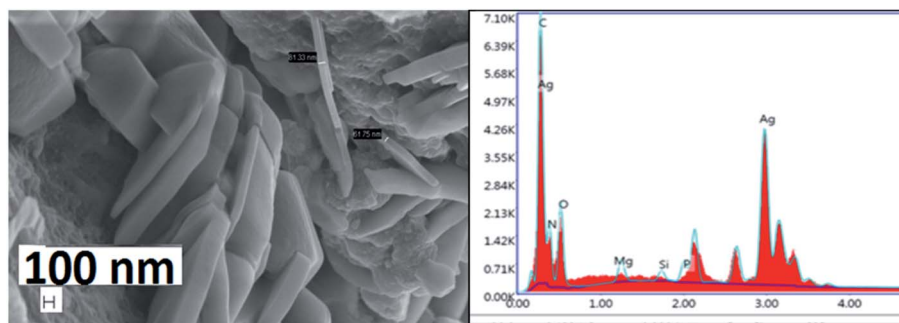

Fig. 11 FESEM/EDX report of freshly synthesized silver nanoplates using *Colocasia esculenta* leaf extract.

The FESEM/EDX images for silver nanoplates synthesized using *Colocasia esculenta* leaf extract (Fig. 11) also showed the formation of hexagonal nanoplates. Some nanoplates were seen to be slightly rounded in the corners which indicate that they were etched at the corners due to unstable environmental conditions. The larger size of nanoplates (in micro meter scale) was due to higher concentration of $AgNO_3$ (0.02 M) compared to that in *Eichhornia crassipes* leaves. The etching can be prevented by keeping the nanoplates in borate buffer solution[26] and desired size can be obtained for a particular application.

HRTEM/SAED images of the synthesized nanoplates were recorded but after about 30 days from the day of synthesis. As expected from other characterizing techniques, some hexagonal nanoplates were observed in Fig. 12. Due to sensitive environment, the edges of hexagonal nanoplates dissolved resulting in

roughly circular shapes with ultimate size approx. 22 nm. This observation is supported by the UV Vis spectra, DLS records as well as powder XRD analysis of the synthesized silver nanoplates.

"The synthesized nanostructures were nanoplates and not nanoparticles" was confirmed from the appearance of two surface Plasmon bands instead of one in UV-Vis spectrum. The characterization results in the present work are also in agreement with the journals reporting the synthesis of silver nanoplates using chemical methods.[27–32] All the three types of plant leaves were super hydrophobic as the reported contact angles for each of the three types of leaf surface was near 160°.[33,34] A certain ratio of some phytochemicals like gallic acid and quercetin present in plant leaves may be responsible for reduction and then stabilization of the nanostructures. In order to confirm the role of these two chemicals, the synthesis of silver nanoplates was tried with synthetic gallic acid and quercetin taken in different ratios in different experiments. Silver nanoplates were successfully formed when these two chemicals were taken in 1 : 1 ratio. The UV Vis spectrum (Fig. 13a) of these synthesized nanoplates show shoulder at 320 nm and a broad peak (400–800 nm) with λ_{max} at around 471.6 nm.

Since $\lambda_{max} < 500$ nm, small silver nanoplates are expected to be formed. The epicuticular wax material over the surface of leaves showing lotus effect contains nonacosanediols and nonacosan-10-ol in varying amount which are expected to behave as templating agent and are responsible for the formation of 2-D structures, the nanoplates of significant size and shape. This assumption was based on the fact that if we use extract of plant leaves which are not super hydrophobic, spherical nanoparticles showing only one SPR peak around 400 nm is observed in UV Vis spectra and no nanoplates are formed. For example if Tulsi (*Ocimum sanctum*) leaves extract is used for the synthesis of silver nanoparticles, only one SPR band near 400 nm is seen confirming the formation of nanoparticles and not nanoplates.[35]
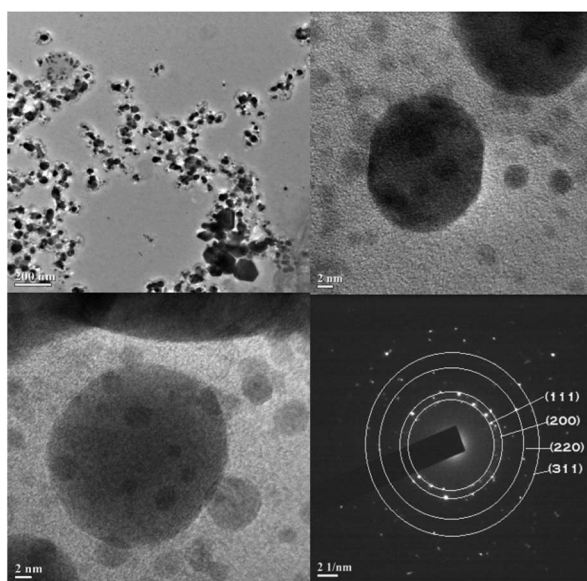

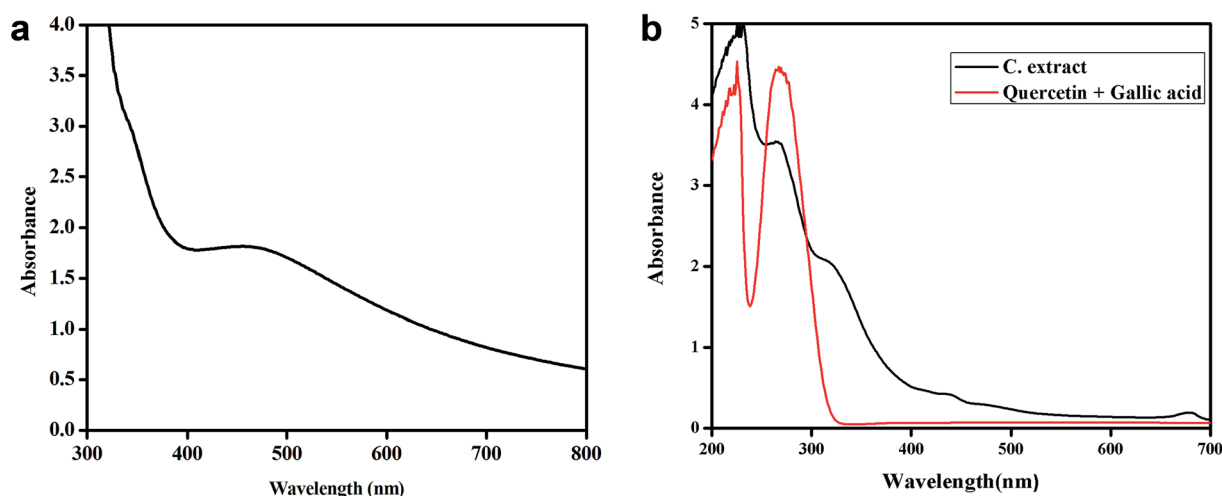**Fig. 12** TEM and SAED images of the synthesized silver nanoplates.

Fig. 13 (a) UV-Vis spectra of silver nanoplates synthesized using gallic acid and quercetin in 1 : 1 ratio. (b) UV-Vis spectra of gallic acid and quercetin in 1 : 1 ratio and *Colocasia esculenta* leaf extract.

The UV-Vis comparison spectra of gallic acid with quercetin in 1 : 1 ratio and *Colocasia esculenta* leaf extract in Fig. 13b shows two peaks which have the similar λ_{max} values for the two, *i.e.* for gallic acid the λ_{max} values are 229 nm and 263 nm and for the leaf extract the peaks are found to be at 229 nm and 264 nm. It clearly shows that gallic acid and quercetin are present in the plant leaves extract which is responsible for reducing Ag^+ to Ag^0 and thus leads to the formation of silver nanoplates. Finally, it was concluded that 1 : 1 ratio of gallic acid and quercetin in the plants leaves showing lotus effect was responsible for the formation and stabilization of silver nanoplates with non-acosanediols and nonacosan-10-ol as templating agent for significant shape and size of the nanoplates.

Preliminary investigation on application of the silver nanoplates synthesized using green method

Silver nanoplates are reported to show better antimicrobial activity than the spherical nanoparticles.[9,11,36] In order to test the preliminary antibacterial activity of silver nanoplates synthesized using plant leaf extract, we applied the test for both Gram positive (*S. aureus* and *B. subtilis*) and Gram negative (*E. coli*) bacteria.

When the antimicrobial activity was checked using 1 mM solution of smaller nanoplates in different volumes, antibacterial activity against *Escherichia coli* and *Bacillus subtilis* was not shown at a concentration of 200 $\mu L\ mL^{-1}$, but for *Staphylococcus aureus*, a Gram positive bacterium, a zone of inhibition of 5 mm was observed using such a low concentration of silver nanoplates. This result of preliminary application shows the possibility of the use of silver nanoplates as antimicrobial agent which will be the next part of our research work.

The larger nanoplates may find applications in SERC (Surface Enhanced Raman Scattering), catalysis *etc.* because of the large surface area. The size control of the nanoplates may be achieved by pouring the nanoplates in borate buffer.

Conclusions

Hexagonal and roughly spherical shaped silver nanoplates have successfully been synthesized using *Eichhornia crassipes* and *Colocasia esculenta* plant leaves extract. This work is the first ever report of green synthesis of silver nanoplates using the leaf extract of a special category of plant showing lotus effect. No external chemical except the precursor was used during the synthesis. The phytochemicals, gallic acid and quercetin along with Si in a certain ratio present in the leaf extract were responsible to reduce and stabilize the synthesized nanoplates. The chemicals in wax covering of the surface of the leaves particularly nonacosanediols and nonacosan-10-ol behave as templating agent and were mainly responsible for the formation of 2-D nanoplates of significant shape and size. The synthesized nanoplates were bigger in size initially but as these nano structures are sensitive to surrounding environment, the edges of the nanoplates dissolves and the hexagonal nanoplates become roughly circular in shape. These silver nanoplates were found to be effective as antibacterial material for *S. aureus*,

a Gram positive bacterium even at very low concentration. Future scope of the work is that the silver nanoplates synthesized following a green route, may be functionalized in different manners in order to enhance their application as antimicrobial agent, sensor *etc.*

Conflicts of interest

There are no conflicts of interest to declare.

Acknowledgements

References

1 R. Jin, Y. Cao, C. A. Mirkin, K. L. Kelly, G. C. Schatz and J. G. Zheng, *Science*, 2001, **294**, 1901–1903.

2 I. P. Santos and L. M. Liz-Marzán, *J. Mater. Chem.*, 2008, **18**, 1724–1737.

3 Y. Zao, Z. Jian-bo, H. Hua, X. Xi-bin, L. Bing-chi, L. Xi-bo, L. Kai, N. Gao, T. Xiu-lan, L. Jiang-shan, T. Yong-jian, W. Wei-dong and Y. You-gen, *Trans. Nonferrous Met. Soc. China*, 2012, **22**, 865–872.

4 Q. Zhang, N. Li, J. Goebl, Z. Lu and Y. Yin, *J. Am. Chem. Soc.*, 2011, **133**, 18931–18939.

5 A. Shahzad, J. Chung, T. J. Lee, Y. H. Kim, S. H. Bhang, W. S. Kim and T. Yu, *ChemistrySelect*, 2018, **3**, 1801–1808.

6 D. M. T. Dang, C. M. Dang and E. F. Blanc, *Internet J. Nanotechnol.*, 2015, **12**(5/6/7), 456–465.

7 M. Jayandran, M. M. Haneefa and V. Balasubramanian, *J. Appl. Pharm. Sci.*, 2015, **5**(12), 105–110.

8 R. Ramanathan, A. O' Mullane, P. M. Smooker, S. K. Bhargava and V. Bansal, *ICONN 2010 978-1-4244-5262-0/10/$26.00 © 2010 IEEE 271–273*.

9 S. Pal, Y. K. Tak and J. M. Song, *J. Appl. Environ. Microbiol.*, 2007, **73**(6), 1712–1720.

10 H. Ichimaru, A. Harada, S. Yoshimoto, Y. Miyazawa, D. Mizoguchi, K. Kyaw, K. Ono, H. Tsutsuki, T. Sawa and T. Niidome, *Langmuir*, 2018, **34**, 10413–10418.

11 J. Djafari, C. Fernández-Lodeiro, A. Fernández-Lodeiro, V. Silva, P. Poeta, G. Igrejas, C. Lodeiro, J. L. Capelo and J. Fernández-Lodeiro, *Front. Chem.*, 2019, **6**, 677.

12 https://nanografi.com/blog/lotus-effect-in-nanotechnology/.

13 H. J. Ensikat, P. Ditsche-Kuru, C. Neinhuis and W. Barthlott, *Beilstein J. Nanotechnol.*, 2011, **2**, 152–161.

14 J. S. L. Serrano, O. M. Rutiaga-Quinones, J. Lopez-Miranda, H. A. Fileto-Perez, F. E. Pedraza-Bucio, J. L. Rico-Cerda and J. G. Rutiaga-Quinones, *BioResources*, 2016, **11**(3), 7214–7223.

15 J. A. Rorong Sudiarso, B. Prasetya, J. Polii-Mandang and E. Suryanto, *Agrivita*, 2012, **34**(2), 152–160.

16 M. Kumar and R. Bhardwaj, *Sci. Rep.*, 2020, **10**, 935, DOI: 10.1038/s41598-020-57410-2.

17 R. Prajapati, M. Kalariya, R. Umbarkar, S. Parmar and N. Sheth, *Int. J. Nutr., Pharmacol., Neurol. Dis.*, 2011, **1**(2), 90–96.

18 S. Chen and D. L. Carroll, *J. Phys. Chem. B*, 2004, **108**(18), 5500–5506.

19 I. Pastoriza-Santos and L. M. Liz-Marzán, *J. Mater. Chem.*, 2008, **18**, 1724–1737.

20 A. Talib and H. F. Wu, *J. Mol. Liq.*, 2016, **220**, 795–801.

21 N. Supraja, B. Avinash and T. N. V. K. V. Prasad, *Adv. Nano Res.*, 2017, **5**(4), 373–392.

22 S. Naz, A. R. Khaskheli, A. Aljabour, H. Kara, F. N. Talpur, S. T. Hussain Sherazi, A. Ali Khaskheli and S. Jawaid, *Advances in Chemistry*, Hindawi Publishing Corporation, 2014, p. 686925, 6 pages, DOI: 10.1155/2014/686925.

23 S. Jain and M. S. Mehata, *Sci. Rep.*, 2017, **7**, 1–13.

24 J. L. Coward, *J. Biol. Phys.*, 2010, **36**, 405–425.

25 S. Kumar, M. Sneha, K. Won, S. W. Cho, C. W. Kim and S. Yun, *Colloids Surf., B*, 2009, **73**, 332–338.

26 https://nanocomposix.com/pages/silver-nanoplates.

27 S. Chen and D. L. Carroll, *Nano Lett.*, 2002, **2**(9), 1003–1007.

28 Y. Zao, Z. Jian-bo, H. Hua, X. Xi-bin, L. Bing-chi, L. Xi-bo, L. Kai, N. Gao, T. Xiu-Lan, L. Jiang-shan, T. Young-jian, W. Wei-dong and Y. you-gen, *Trans. Nonferrous Met. Soc. China*, 2012, **22**, 865–872.

29 Y. M. Park, B. G. Lee, J. Weon and M. H. Kim, *RSC Adv.*, 2016, **6**, 95768.

30 G. C. J. Swarnavalli, V. Joseph, V. Kannappan and D. Roopsingh, *J. Nanomater.*, 2011, 5, DOI: 10.1155/2011/825637.

31 A. U. Khan, Z. Zhou, J. Krause and G. Liu, *Small*, 2017, 1701715.

32 R. Fan, Y. Yang, J. Xue, F. Zhang, J. Sun, H. Xu and T. Jiang, *ChemNanoMat*, 2020, **6**, 148–153, DOI: 10.1002/cnma.201900603.

33 H. Wang, H. Shi and Y. Wang, The Wetting of Leaf Surfaces and Its Ecological Significances, *Wetting and Wettability*, ed. M. Aliofkhazraei, IntechOpen, 2015, DOI: 10.5772/61205.

34 E. Papierowska, S. Szporak-Wasilewska, J. Szewińska, J. Szatyłowicz, G. Debaene and M. Utratna, *Trees*, 2018, **32**, 1253–1266.

35 C. Ramteke, T. Chakrabarti, B. K. Sarangi and R. A. Pandey, *J. Chem.*, 2013, 278925, DOI: 10.1155/2013/278925.

36 B. Sadeghi, F. S. Garmaroudi, M. Hashemi, H. R. Nezhad, A. Nasrollahi and S. Ardalan, *Adv. Powder Technol.*, 2012, **23**(1), 22–26.